Acta Geologica Sinica (English Edition), 2019, 93(6): 1662–1672

Quantitative Prediction of Fracture Distribution of the Longmaxi Formation in the Dingshan Area, China using FEM Numerical Simulation

XIE Jiatong[1, 2, *], QIN Qirong[1, 2] and FAN Cunhui[1, 2, 3]

[1] *State Key Laboratory of Oil and Gas Reservoir Geology and Exploitation, Southwest Petroleum University, Chengdu 610500, China*
[2] *School of Geoscience and Technology, Southwest Petroleum University, Chengdu 610500, China*
[3] *Collaborative Innovation Center of shale gas resources and environment,Southwest Petroleum University, Chengdu 610500, China*

Abstract: Fracture prediction is a technical issue in the field of petroleum exploration and production worldwide. Although there are many approaches to predict the distribution of cracks underground, these approaches have some limitations. To resolve these issues, we ascertained the relation between numerical simulations of tectonic stress and the predicted distribution of fractures from the perspective of geologic genesis, based on the characteristics of the shale reservoir in the Longmaxi Formation in Dingshan; the features of fracture development in this reservoir were considered. 3D finite element method (FEM) was applied in combination with rock mechanical parameters derived from the acoustic emissions. The paleotectonic stress field of the crack formation period was simulated for the Longmaxi Formation in the Dingshan area. The splitting factor in the study area was calculated based on the rock breaking criterion. The coefficient of fracture development was selected as the quantitative prediction classification criteria for the cracks. The results show that a higher coefficient of fracture development indicates a greater degree of fracture development. On the basis of the fracture development coefficient classification, a favorable area was identified for the development of fracture prediction in the study area. The prediction results indicate that the south of the Dingshan area and the DY3 well of the central region are favorable zones for fracture development.

Key words: FEM numerical simulation, structural stress field, fracture prediction, Longmaxi Formation

Citation: Xie et al., 2019. Quantitative Prediction of Fracture Distribution of the Longmaxi Formation in the Dingshan Area, China using FEM Numerical Simulation. Acta Geologica Sinica (English Edition), 93(6): 1662–1672. DOI: 10.1111/1755-6724.13815

1 Introduction

In recent years, a variety of fracture prediction methods have been widely applied, among which the finite-element numerical simulation of the tectonic stress field is the most commonly used (Zhang et al., 2004; Wei et al., 2006; Xie et al., 2008; Zhou et al., 2009; You, 2010; Ding et al., 2010, 2011, 2016). The tectonic stress field is a geostress field that is related to geological tectonic movement, which, in general, refers to the geostress field that causes tectonic movements. It can be analyzed to characterize the origin of regional tectonic movements, as well as the spatiotemporal distribution and force source of the stress field. Using this kind of analysis, tectonic movement rules and forms can be expressed directly, completely, and uniformly (Liu, 2002). Fracture development is closely related to the tectonic stress field and fault structure.

A number of studies have been undertaken to investigate the relationship between the tectonic stress field and fracture development in oil and gas reservoirs (Shen, 2008; Tang et al., 2012; Zhang, 2014; Lu et al., 2016). The method of numerical simulation of the tectonic stress field is the most effective way to achieve the quantitative description of reservoir structural fractures, and many explorations have been made, that verify the capacity of tectonic stress field simulations for predicting favorable zones with developed fractured reservoirs (Zhou et al., 2003; Qin et al., 2004; Liu et al., 2008; Wang et al., 2009). Most previous studies focused on the description of core fractures. Because no reasonable mechanical model has been established, the fractures in the reservoir scope can only be predicted qualitatively and semi-quantitatively. In addition, there is a lack of systematic means and methods to establish the quantitative relationship between the stress–strain and fracture parameters according to the numerical simulation of the stress field in ancient and modern times, and it is difficult to accurately calculate the fracture parameters in the study area. Tectonic stress field simulations encounter two main difficulties because the object of the simulation is often a very complicated subsurface geological body. (1) There are various types of geological events in the long geological evolutionary history, but such complex geological evolution cannot be fully reconstructed; (2) the widely distributed and deeply buried reservoir layers exhibit complex heterogeneity

* Corresponding author. E-mail: 963955769@qq.com

owing to the influences of many factors on the rock physical properties. To better simulate the stress field, relatively static viewpoints and methods are employed to address rock mass-related issues, and relatively uniform rock masses are used to approximate the actual geological bodies to minimize the deviation from the actual geological conditions (Zeng et al., 2013; Zhang et al., 2015; Wei et al., 2016; Fang et al., 2017; Lv et al., 2017).

In the Longmaxi Formation, Dingshan area, the fracture system and fracture development characteristics are identified through comprehensive geological analyses, including acoustic emission-based geostress measurements and rock mechanical parameter analysis and consideration of the effect of faults on fracture formation. Moreover, according to the fracture formation mechanism, elasticity theory, and rock fracture criteria, a three-dimensional finite-element method is introduced to simulate the paleotectonic stress field of the Longmaxi Formation in the Dingshan area from the Late Yanshanian period to the middle period of Himalayan tectonic movement (Fan et al.,2018). Finally, areas with favorable distributions and fracture development are predicted in the study area (Niu et al., 2006; Zhu, 2013; Yuan, 2014; Wang et al., 2016).

2 Geological Setting

The Dingshan area is located in the southeastern part of the Sichuan Basin at the junction of Xishui County, Guizhou Province, and Qijiang, Chongqing. The Dingshan area is affiliated with Shihao Town of Qijiang County, Chongqing. The Dingshan structure is located at the junction of the high and steep fold zone of southeast Sichuan in the southeastern part, the eastern margin of the low fold zone across southern Sichuan, and the slope zone of southern Sichuan in the southern part of the Sichuan Basin. At the margin of the basin, a thrust nappe structure was formed under the control of the Qiyueshan faults (Yuan et al., 2008; Mei et al., 2010; Huang et al., 2017). The Dingshan structure was subject to the influence of multi-episodic tectonic movement since the Yanshanian period, and the direction of its tectonic stress experienced multi-episodic change. The overall form on the plane exhibits a NE-SW-trending nasal anticline (Fig. 1a). Affected by the Xuefeng uplift, central Sichuan uplift, and central Guizhou uplift, the research region has a complicated tectonic structure, a varied morphology, and developed folds and faults. The main structure is mainly the trough folds composed of a series of NE-trending and NNE-trending high and steep anticlines and fault zones and has the characteristics of narrow synclines and wide anticlines. The Devonian, Carboniferous, and other later Mesozoic strata are generally absent in the regional strata. The strata in the core part of the anticline are seriously denuded, causing the relatively old Sinian strata to be exposed to the ground surface; the old Sinian strata continues to suffer varying degrees of weathering and denudation even now. Because of the Jiangnan-Xuefeng uplift, the central Sichuan uplift and central Guizhou uplift were formed in the Upper Yangtze region and exposed at sea level during the early stage of the Late Ordovician-Early Silurian period. These three uplifts surround the Sichuan Basin and peripheral rim. Because the Early-Middle Ordovician open sea was transformed into a confined shallow sea with relative retention, a large area, low energy, and an anoxic strong reduction depositional environment, confined by the three uplifts, a set of high-quality black shales rich in organic matter and graptolite, which is called the Wufeng Formation-Longmaxi Formation and has a thickness greater than 30 m, was deposited (Fig. 1b).

3 Methods and Descriptions

In the quantitative prediction of fracture distribution, the fracture development distribution in the study area is predicted by the combination of geological method and numerical simulation, and by using the criterion of rock fracture strength. In the geological method, the field outcrop fractures and downhole fractures are observed and counted respectively, the density, angle and orientation of the fractures are determined, and the rock mechanics experiments are prepared. In the numerical simulation method, the finite element method (FEM) combined with the experimental parameters of rock mechanics is mainly used to constrain the boundary conditions and load the force on the model of the study area. Finally, the fracture distribution of the study area is quantitatively predicted by using the rock fracture strength criterion.

3.1 Finite element numerical simulation

After decades of development, various rock mechanics methods have been developed, such as the finite-element method, boundary element method, finite-difference method, discrete element method, manifold element method, Lagrange element method, discontinuous deformation method, and element-free method. Each of these methods has their own advantages and disadvantages.The theoretical basis and application of the finite-element method are mature, and its application for the calculation of metal materials and components has been very successful. However, it is based on a continuous medium and appears to be far from the discontinuity of the rock mass. Although the manifold element method considers the effect of fractures in the rock mass, its theoretical basis is not mature (Cao et al., 2009; Wang et al., 2017).

The finite-element method can address the problems of mechanics and partial differential equations with special boundary conditions in mathematics, which is suitable for the analysis of geomechanics. In fracture development predictions, the three-dimensional finite-element method can be used to numerically simulate tectonic stress fields, in which continua are hypothetically divided into a finite number of discrete elements, and these sets of discrete elements are used to replace the original continua (Shen et al., 2008). The research object of a finite-element numerical simulation is an approximate model, whereas that of this geological study is an underground objective entity. Therefore, the finite-element numerical simulation method can be coupled with the geological model for fracture prediction, and the resulting model is expected to

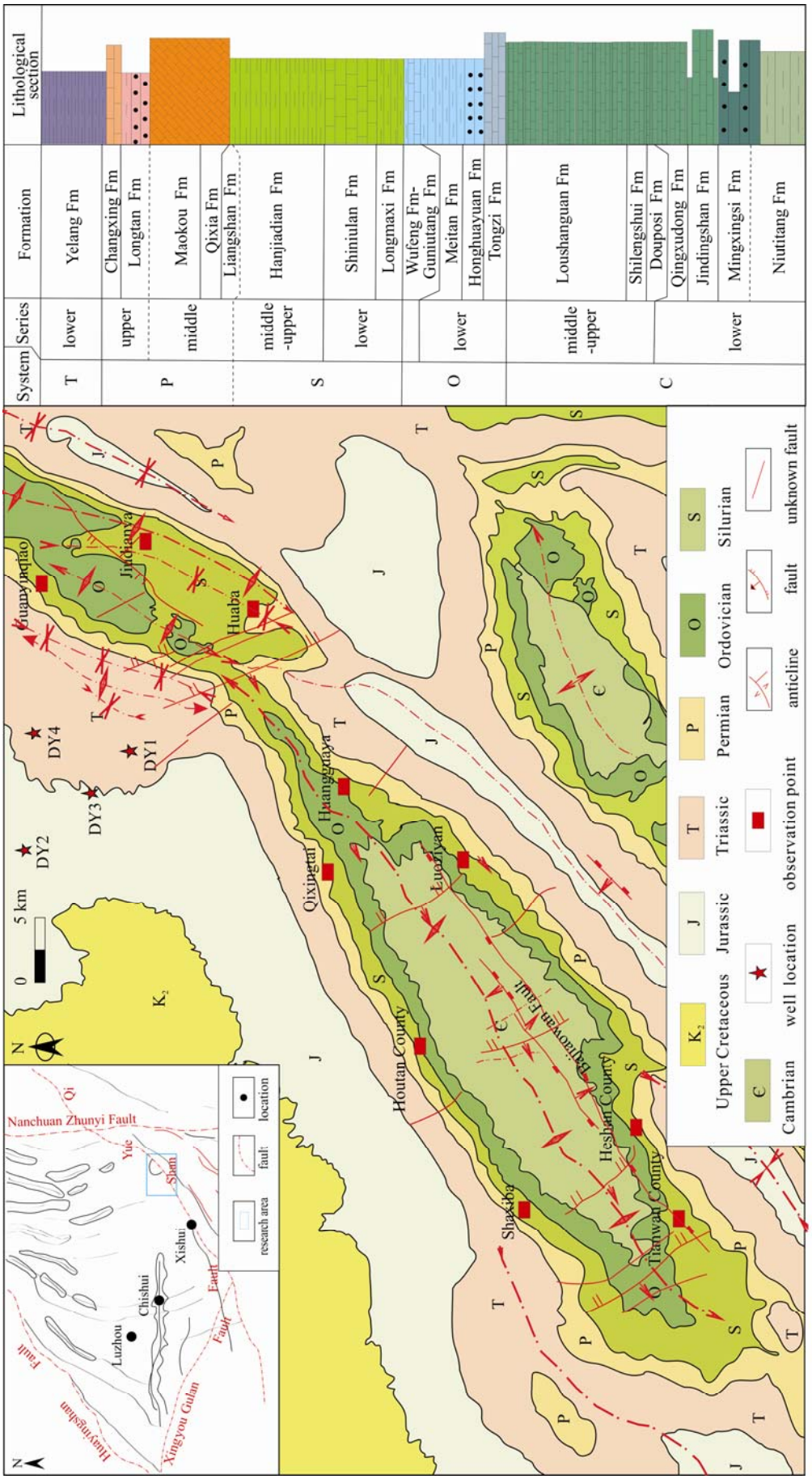

Fig. 1. Tectonic division of southeast Sichuan and the location of the Dingshan area (a) and the lithology of Longmaxi Formation (b).

objectively reflect the characteristics of the underground entity.

3.2 Prediction methods

According to rock mechanical theory, there are four categories of fracture strength theories for characterizing rock failure conditions: the maximum tensile strain theory, Mohr's strength theory, the strength theory of shear strain energy, the octahedral stress theory, and the Griffith theory. Each theory can be divided into different criteria, which are exclusively applicable to different environmental conditions. As shale gas reservoirs are generally deeply buried and have a high confining pressure, the Mohr–Coulomb criterion can be used for rock fracture determination (Qin et al., 2004; Yin et al., 2014).

According to Mohr's theory, the rock failure approach index can be simply expressed as $\eta=f(\sigma)/\mathrm{K}(\kappa)$, and the physical meanings of the parameters are shown in Fig. 2.

The specific expression is

$$\eta = \frac{f}{k} = \frac{\sigma_1 - \sigma_2}{(\frac{c}{\tan\phi} - \frac{\sigma_1 + \sigma_2}{2})\sin\phi} \quad , \tag{1}$$

Here, σ_1 and σ_2 are the maximum and minimum principal stresses, respectively, during the tectonic movement. The stresses are perpendicular to each other, and the unit is MPa. c is the cohesion of the rocks. A greater cohesive force indicates a greater force between the two molecules and a lower likelihood of fracture. φ is the internal friction angle of the rocks.

In theory, when $\eta \geqq 1$, fractures occur. Larger values of η correspond to a higher fracture intensity and thus more developed fractures. When $\eta < 1$, the rock is stable, and fractures are not developed. However, the actual situation is often more complex than this; thus, other factors should be considered in the evaluation.

The c and φ values reflect the state of molecular cohesion within the rock, as well as the rock brittleness. Therefore, they are important factors in the study of rock fractures.

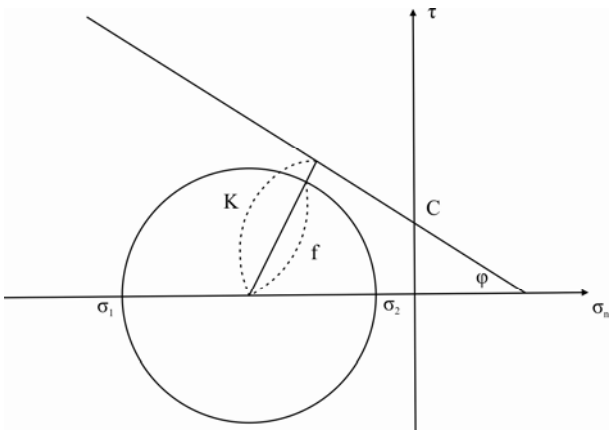

Fig. 2. The Mohr - Coulomb model schematic diagram using failure approach index.

4 Analytical Results

4.1 Fracture system and fracture development characteristics

4.1.1 Fracture system

The fault structure of Longmaxi Formation in the Dingshan area developed mainly in the NE and NNE directions (Fig. 3). The NNE fault was mainly formed in the middle and late Yanshanian period and intersected with the high angle of the plane. When the inclination angle is above 75°, the shear fractures in the NNE profile are formed under the near-SN tectonic compression. The NNE trending faults were formed by the compression in the NNE direction from the late Yanshanian period to the middle period of Himalayan tectonic movement. With the continuing action of the NE tectonic forces, the NW shear fractures perpendicular to the principal stress direction were formed in the already folded and deformed strata. A large fault was formed near the DS1 and DY4 wells, which is the main fault direction controlling the development and distribution of fractures in the Dingshan area (Wei et al., 2017).

4.1.2 Fracture development characteristics

(1) Outcrop crack

By observing the fractures of Longmaxi Formation in the Dingshan area and the surrounding outcrops, it is found that the main types of outcrop fractures in the field are shear fractures (Fig. 4), with vertical or high-angle plane shear fractures and low-angle profile shear fractures. The plane shear fracture intersects with the vertical or high angle of the rock plane. It is formed early and widely distributed. The fracture surface is straight, and the occurrence is stable (Fig. 4a). The cross-sectional shear fracture intersects with the low angle of the rock plane (Fig. 4b), and the formation time is later than that of plane shear fracture. The fractures in the study area are mainly high-angle fractures. The vertical fractures with a dip angle greater than 75° account for 63.72% of the total observed fractures, the high-angle fractures with a dip angle of 45°–75° account for 34.76%, and the low or horizontal fractures are not developed, accounting for only 1.52%. The extension length was small, of which 22.5% is less than 1 m and 32.6% is between 1–2 m. For 74.4% of the total observed cracks, the fracture density is less than 1 m. The cracks with a distance of 1–3 m-mainly cut layer fractures and inner layer cracks-account for 19.4%, and the cracks with a spacing greater than 3 m are not developed, accounting for only 6.2%. The linear density of the fracture is medium, mainly 3–8 m/strip, accounting for 73.6% of the total observed cracks.

(2) Underground fracture

The core can accurately reflect the appearance of underground strata. The observation and description of core fractures is the basic method of fracture research. The degree of fracture development is an important factor controlling the productivity of fractured reservoirs, and it is generally evaluated via measurements of the fracture density, width, and length. Through the observation of five coring well fractures in Longmaxi Formation in the Dingshan area, it is found that the fractures in the study

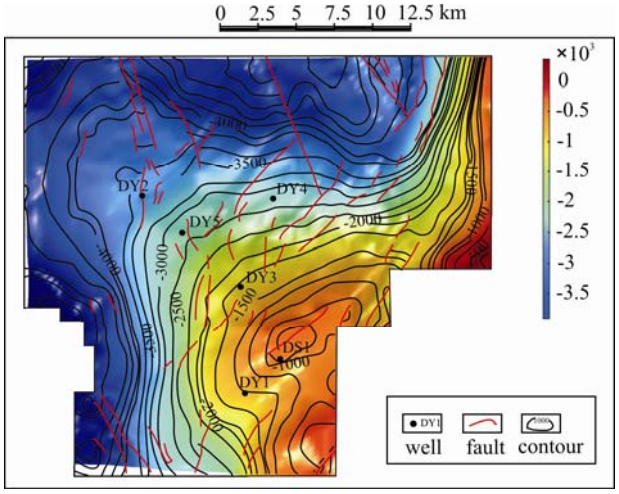

Fig. 3. The top surface structural map of the Longmaxi Formation in the Dingshan area

area are generally developed, have various types, and are mainly structural fractures formed by tectonic action. Diagenesis fractures formed by diagenesis and a small amount of artificially induced fractures during drilling or production. Structural fractures are mainly shear fractures, followed by tensile fractures, bedding fractures, reticular fractures, and slippage fractures (Fig. 5). Among them, the shear fractures are mainly high-angle fractures and vertical fractures, which have the characteristics of a large extension length and a straight face, and most of them are filled with calcite. The ductile shear fracture of shale, which is rich in brittle minerals, occurs under the action of local or regional tectonic stress, forming high-angle shear fractures and tensional fractures, which are often associated with faults or folds (Fig. 5a). Tensional fractures usually have a small extension length, are irregular in the plane, and are filled with calcite (Fig. 5b), and bedding fractures are mostly horizontal fractures (Fig. 5c). Different types of fractures

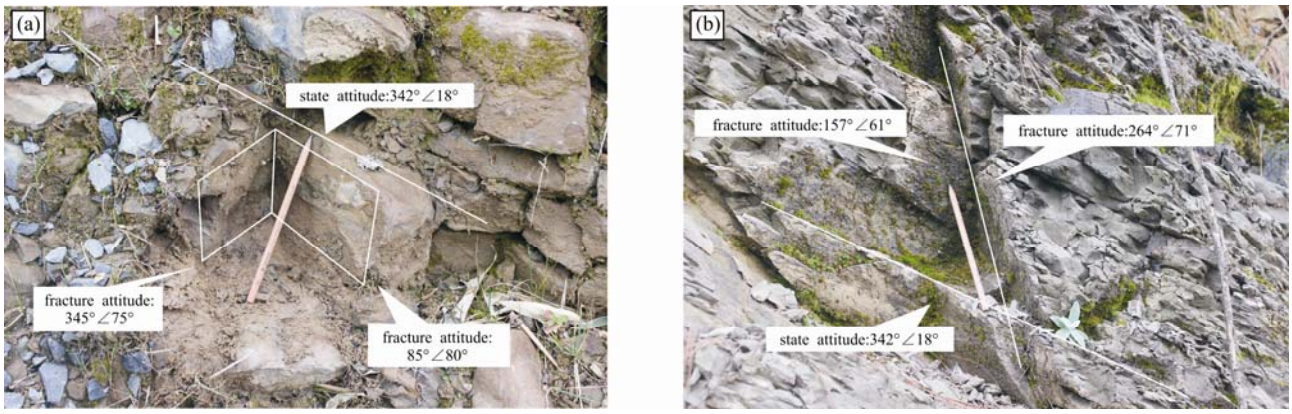

Fig. 4. Outcrop profile of Shale of the Longmaxi Formation in the Dingshan area.
(a) Plane shear fracture; (b) section shear fracture.

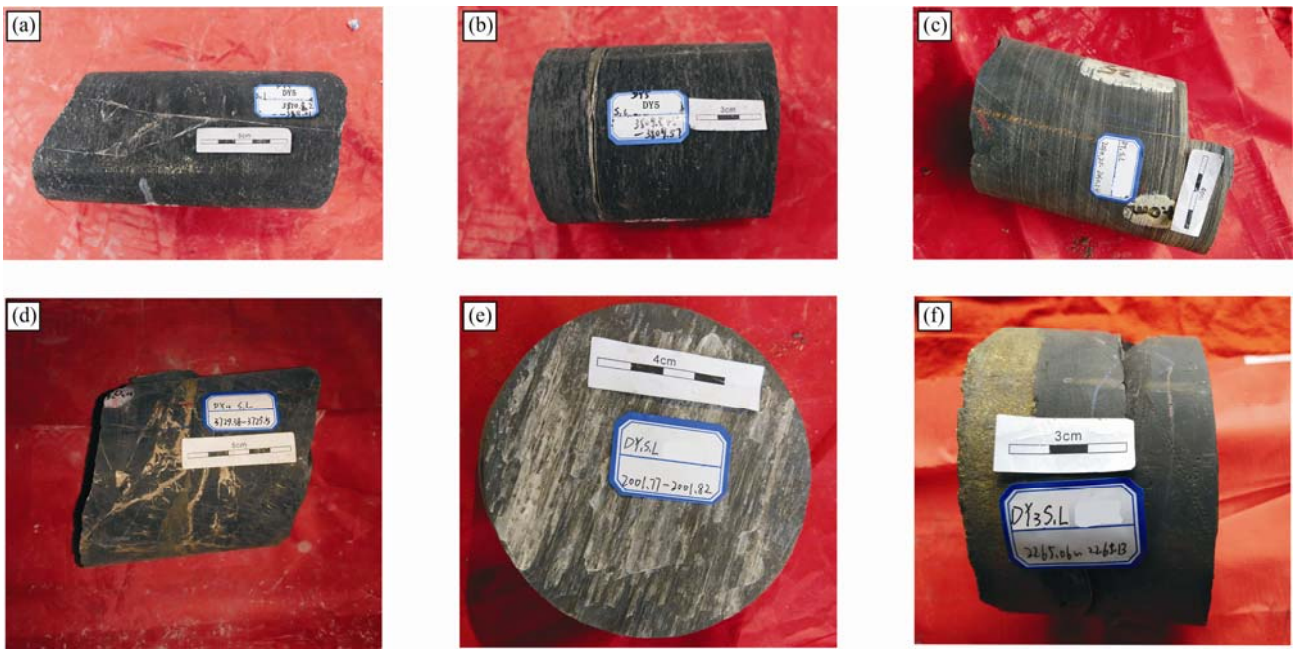

Fig. 5. Photographs of shale core fractures of the Longmaxi Formation in the Dingshan area
(a) High angle shearfracture (DY5:3810.82-3811.01m); (b) calcite half filling (DY5:3809.45-3809.57m); (c) horizontal fracture (DY1:2030.25-2030.34m); (d) reticular fracture (DY4:3729.38-3729.5m); (e), scratch (DY1:2001.77-2001.82m); (f) interlaminar fracture (DY3:2265.06-2265.13m).

interweave to form reticular fractures (Fig. 5d), which is an important fracture type in the study area and plays an important role in the improvement of the reservoir percolation ability. The occurrence of slippage fracture is basically consistent with that of rock strata, with small inclination, a large tendency, an uneven face, and visible scratches (Fig. 5e), and interlayer fractures are usually filled with calcite, pyrite, and organic matter (Fig. 5f).

As observed in the fractured cores of the Longmaxi Formation, most fractures have low angles (15°–45°) or high angles (45°–75°), medium extensions (mainly 10–20 cm), a high degree of closure, small widths (mainly 0.1–1 mm).The degree of fracture filling is high, 50% of the total filling fractures and 50% of the half-filled and unfilled fractures (Fig. 6).

4.2 Finite element numerical simulation

4.2.1 Boundary conditions

In simulations of tectonic stress field, two kinds of boundary conditions are adopted, namely, the boundary condition of stress and the boundary condition of displacement. Moreover, the stress on the boundary is assumed to be evenly distributed. Based on rock acoustic emission experiments and geostress equations (Eqs. 2–4), the value and direction of the maximum effective paleostress that the Longmaxi Formation shale once experienced can be obtained:

$$\sigma_H = \frac{\sigma_{0^\circ} + \sigma_{90^\circ}}{2} + \frac{\sigma_{0^\circ} - \sigma_{90^\circ}}{2}\left(1 + tg^2 2\alpha\right)^{\frac{1}{2}} + \beta P_p \ , \quad (2)$$

$$\sigma_h = \frac{\sigma_{0^\circ} + \sigma_{90^\circ}}{2} - \frac{\sigma_{0^\circ} - \sigma_{90^\circ}}{2}\left(1 + tg^2 2\alpha\right)^{\frac{1}{2}} + \beta P_p \ , \text{ and} \quad (3)$$

$$tg2\alpha = \frac{\sigma_{0^\circ} + \sigma_{90^\circ} - 2\sigma_{45^\circ}}{\sigma_{0^\circ} + \sigma_{90^\circ}} \ , \quad (4)$$

where β is the effective stress factor; P_p is the formation pore pressure; σ_v is the overlying strata stress; σ_H and σ_v are the maximum and minimum horizontal principal stresses, respectively; σ_0, σ_{45°, and σ_{90° are the stresses at the Kaiser points of the cores obtained at horizontal coring directions of 0°, 45°, and 90°, respectively; and α is the azimuth of the maximum horizontal principal stress, where the stress and pressure units are both MPa.

Through acoustic emission experiments, it has been clarified that the Dingshan Area experienced northeastern and southeastern compression during the late Yanshanian to middle period of Himalayan tectonic movement. Accordingly, the stress boundary conditions were set to a positive stress of 100 MPa in the northeast and a positive stress of 75 MPa in the southeast. Given the self-weight of the model strata, the top surface of the model was considered to bear a uniform load, which is the weight of the overlying strata. The average cumulative depth from the model top to the ground surface is 2,000 m. A vertical stress of 52 MPa was imposed on the model top surface, and a counteracting stress of 57 MPa from the underlying strata was imposed on the bottom of the model bottom surface. Because the exact action mode of the stresses on the boundary is unknown, stresses there were regarded to be evenly distributed. For the displacement boundary

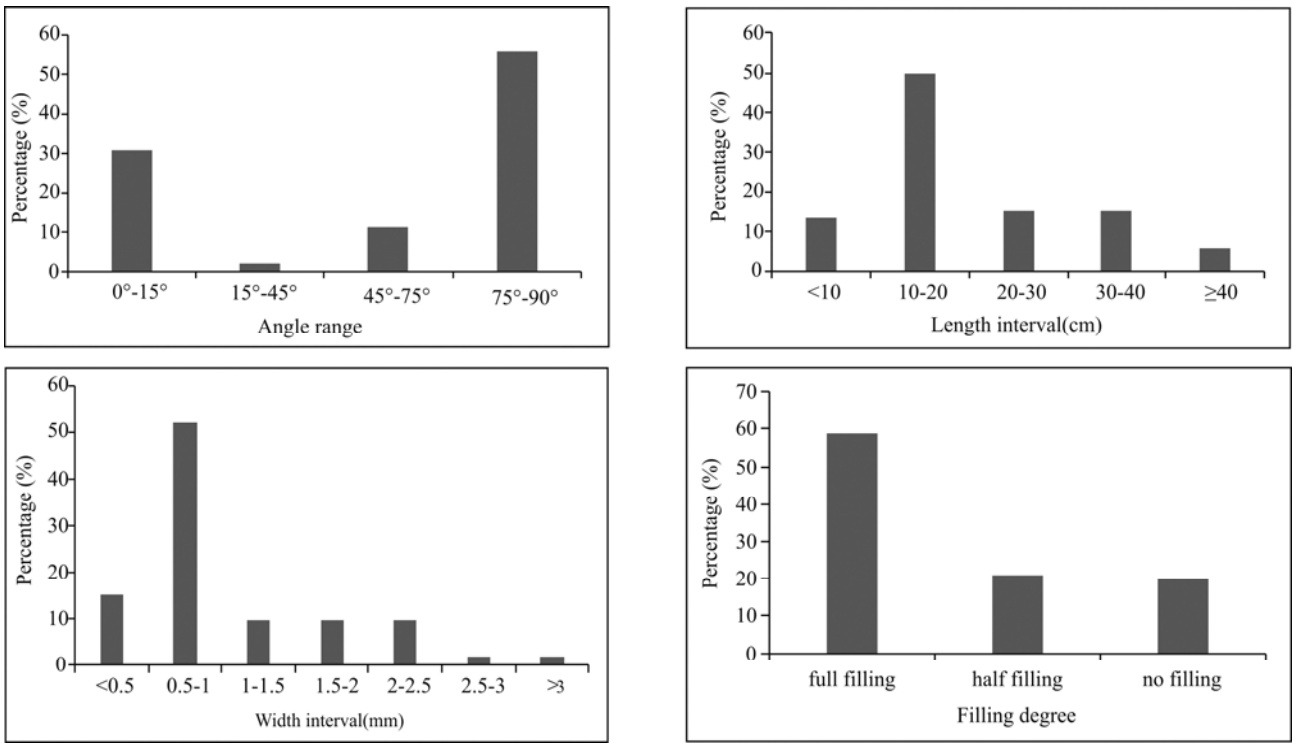

Fig. 6. The core fracture characteristics statistical diagram of the Longmaxi Formation.
Distribution of fracture dip frequency diagram; The distribution of crack length frequency diagram; The distribution of crack width frequency diagram; Crack filling degree distribution frequency diagram.

conditions, the northwestern and southwestern parts were fixed, and the XYZ displacement and rotation angle were set to zero (Fig. 7).

4.2.2 Rock mechanical parameters

Rock mechanical parameters are necessary for tectonic stress field interpretation, and their accuracies are directly related to the reliability of final simulation results. Rock mechanical parameters in different locations of the study area differ due to the differences in the tectonic sites and fault zones. Accordingly, two main kinds of parameters were used in the simulation. In addition to the experimental data, fault and fold zones also needed to be specifically separated, as their deformation and misalignment can result in changes to rock mechanical parameters. In this context, better results can be achieved by individually assigning reasonable mechanical parameters to faults and folds for the geological simulation.

(1) Experimental parameters

Assuming that the block surrounded by faults is continuous, weighted-average simulation parameters for the study area of the Longmaxi Formation, Dingshan area, which has significantly developed fractures, can be determined according to the rock mechanical properties of core samples from wells DY1, DY2, DY3, and DY4 (Table 1). The elastic modulus is 35.29 GPa, the Poisson's ratio is 0.256, the density is 2.596 g/cm^3, the cohesion is 2.78 MPa, and the internal friction angle is 25.73°.

(2) Parameters of fault and fold zones

According to a statistical analysis of the simulated area, grid units distributed in the fault structural plane were statistically calculated, and then they were individually assigned values differing from those of the surrounding rocks to perform the fault simulation (Ding et al., 2010; 2016). This process is referred to as fault weakening. Faults and the surrounding geological body are regarded as mutually continuous materials, and they differ in certain material parameters.

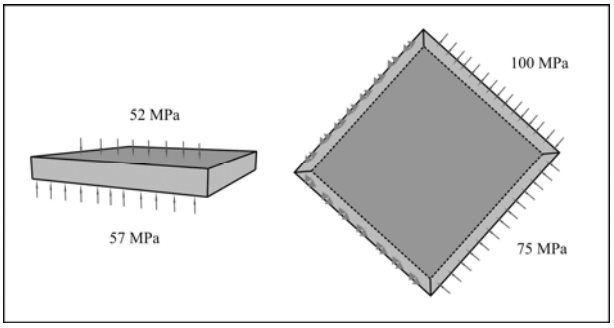

Fig. 7. At the end of the Yanshanian-middle Himalayanian simulation diagram of the Longmaxi formation in the Dingshan area.

On the basis of a triaxial stress experiment, the fault and fold regions were strengthened and weakened to different degrees. The fault material parameters were treated as follows: ① before the formation of the structure, the fault material parameters were weakened, including the reduced elastic modulus (70%–80% of that of the normal area) and the slightly increased Poisson's ratio (0.02–0.1 larger than that of the normal area); and ② the fold zone in the structurally high area was highlighted as a hard zone to ensure similarity between the model and the actual geological conditions, and the fold zone was therefore strengthened, with a larger elastic modulus and smaller Poisson's ratio (0.01–0.11) than other areas (Table 2). According to the simulation of the Dingshan area, the material parameters of faults and folds can be determined when the well location of the simulation results is close to that of the actual well logging results.

5 Discussion

5.1 Tectonic stress field distribution

The Abaqus software was used to simulate the three-dimensional tectonic stress field before fault formation in the Longmaxi Formation, Dingshan area. The distributions of the maximum and minimum principal stresses in the Longmaxi Formation, which are the main factors controlling the degree of fracture development in the formation, were then identified (Dong et al., 2018).

After a large number of simulation trials, preliminary simulation results were obtained with the aim of revealing the tectonic stress field after the formation of structures from the Late Yanshanian period to the middle period of Himalayan tectonic movement. Rocks were found to be strongly fractured in the fault and fold zones under the constant northeastern tectonic compression. It was noticed that stress concentration occurs before faulting. Therefore, the maximum principal stresses in the fault proximity and the northeastern structural ridge are higher than that in the low area, with the stresses ranging from approximately

Table 1 At the end of the Yanshanian- middle Himalayan rock mechanics parameter table

Well	Lithology	Poisson ratio (μ)	Elastic modulus/E (Mpa)	Cohesive force/c (Mpa)	Internal friction angle/ø (°)	Density (g/cm^3)
DY1	Black silty mudstone	0.238	40321.0	3.43	16.73	2.7
	Black carbonaceous shale	0.249	34515.1	2.55	35.55	2.65
	Pale limestone	0.247	30256.9	2.82	27.78	2.63
DY2	Black silty mudstone	0.268	43562.0	3.43	16.73	2.52
	Black carbonaceous shale	0.326	41859.2	2.03	35.02	2.53
	Pale limestone	0.247	30256.9	2.82	27.78	2.54
DY3	Black silty mudstone	0.245	35850.0	3.43	16.73	2.64
	Black carbonaceous shale	0.263	34457.0	2.68	31.41	2.55
	Pale limestone	0.247	30256.9	2.82	27.78	2.6
DY4	Black silty mudstone	0.240	37562.0	3.43	16.73	2.64
	Black carbonaceous shale	0.258	34345.1	2.34	28.78	2.55
	Pale limestone	0.247	30256.9	2.82	27.78	2.6

Table 2 The fracture and fold belt rock mechanics parameter table

Unit type		Elastic modulus/E (Mpa)	Poisson ratio	Cohesive force/c (Mpa)	Internal friction angle/ø (°)
Fracture zone	major fracture	27500	0.263	0.9	15
	Fault zone peripheral	26937	0.258	1	21
	small fault	26783	0.254	1.2	20
Fold zone	Structural ridge	40157	0.247	1.7	24
	Ridge of peripheral	39870	0.241	2.2	25

131.3 to 272.8 MPa. The overall maximum principle stresses are evenly distributed within the range of −151.80 to 343.6 MPa (Fig. 8), whereas the minimum principle stresses are mainly in the range of −32.75 to −181.3 MPa (Fig. 9). The maximum principal stresses in the vicinities of wells DY2, DY3, and DY4 are 71.83, 62.62, and 109.23 MPa, respectively, and the minimum principal stresses are −42.74, −39.73, and −91.23 MPa, respectively. The stress field simulation results are consistent with the actual structural deformation characteristics in the study area.

5.2 Fracture simulation distribution

The rock fracture intensity in the study area was simulated through analysis of the maximum and minimum principal stresses derived from the stress field simulation, as well as the rock fracture intensity equation. The same rock mechanical parameters used for the stress field simulation were assigned, and a rock fracture intensity was constructed (Fig. 10). According to the simulation results, rocks were overall strongly and extensively fractured under the tectonic stress from the Late Yanshanian period to the middle period of Himalayan tectonic movement, with maximum and minimum rock failure approach indices of 1.904 and 0.672, respectively. The rock failure approach indices in most areas, with the exception of the boundary, range from 0.896 to 1.792, and are close to or greater than the threshold value for fracturing.

According to the foregoing comprehensive analysis, high failure intensities mainly occur in the fault development area, the structurally high area in the vicinity of well DS1, and the southwestern fault area. Fractures in these areas mainly occur in the strip and arc forms around the faults that strike nearly northwest, northwest, and northeast, with failure approach indices as high as 1.456-1.568 in the fault and fold zones. In contrast, the failure approach indices in the structurally low and gentle areas in the northwest are generally <0.900.

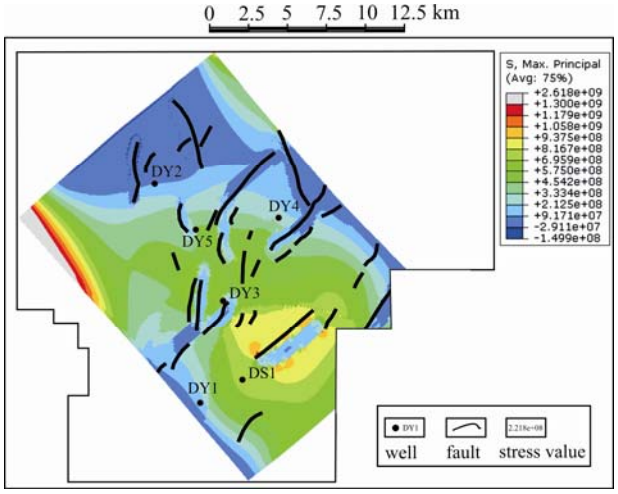

Fig. 8. At the end of the yanshan-Himalayan medium model of maximum principal stress simulation results.

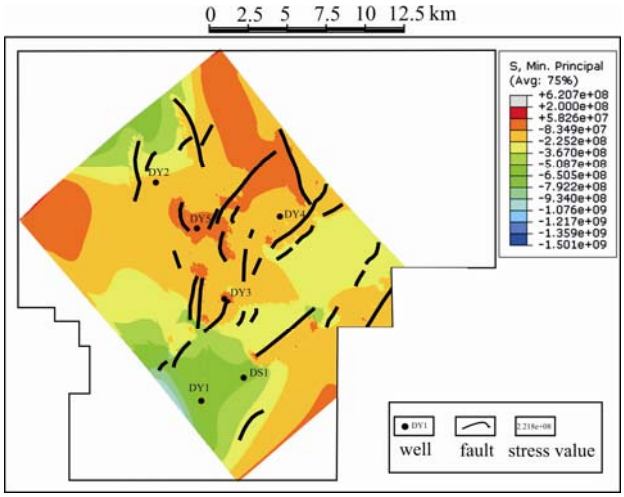

Fig. 9. At the end of the yanshan-Himalayan medium model of minimum principal stress simulation results.

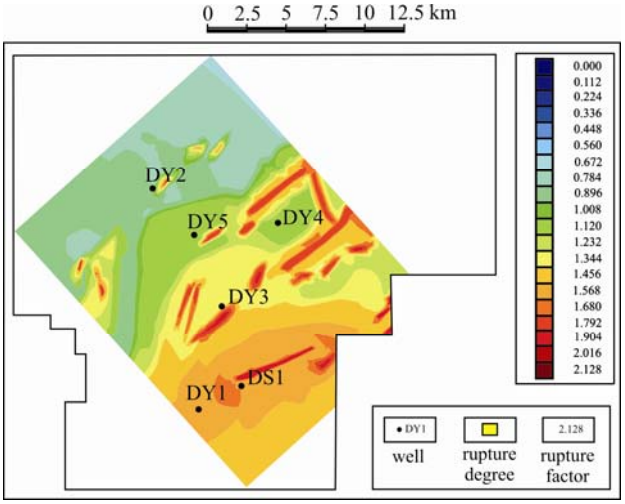

Fig.10. At the end of the yanshan-middle Himalayan rock rupture degree simulation diagram of Longmaxi formation in Dingshan area.

5.3 Quantitative prediction of fracture distribution

The tectonic stress field, strain field, and rock fracture deformation results obtained from the tectonic movement simulation were combined with geological and structural

characteristics as well as experimental tests in the study area. According to the results, five levels of fracture development were identified: the failure zone, strong fracture development zone, moderate fracture development zone, critical fracture development zone, and fracture-free zone (Table 3).

According to the prediction model of fracture development in the Longmaxi Formation, Dingshan area (Fig. 11), the distribution of fractures from the late Yanshanian period to the middle period of Himalayan tectonic movement has the following features.

(1) The fracture zone is mainly distributed near the north–south-striking, northeast-striking, and northwest-striking fault zones. Northeastern and southeastern compressions contribute to large failure approach indices in the fracture zone, all of which exceed 1.792. This is the most significantly fractured zone in the study area, with a maximum failure approach index of 2.016. In the fault zone, the fractures are mainly fault-associated shear fractures, and they are acutely angled with the fracture extension direction, striking nearly south-north, northwest, and northeast.

(2) The Level I fracture development zone is mainly distributed around the periphery of the fault and near the structurally high local areas. The fractures in this zone are strip-like along both sides of the fault, and they have high failure approach indices, which are generally >1.568. They can be high-angle shear fractures, low-angle shear fractures, or high-angle tensile fractures that strike northwest, northeast, and occasionally near SN direction.

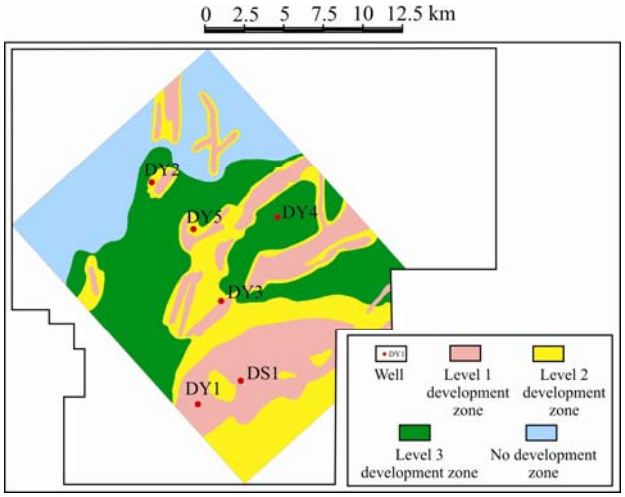

Fig. 11. Fracture development comprehensive forecast figure of Longmaxi formation in Dingshan area.

Table 3 The values of the failure approach index η for prediction of rock fractures in the Longmaxi Formation, Dingshan Area

η value	Fracture intensity	Fracture development level
<0.742	Fracture-free zone	Ⅳ
0.742–1.037	Critical fracture development zone	Ⅲ
1.037–1.332	Moderate fracture development zone	Ⅱ
1.332–1.553	Strong fracture development zone	Ⅰ
≥1.553	Failure zone	Fracture zone

(3) The Level II fracture development zone is mainly located at the periphery of the Level I fracture development zone, in the vicinity of adjacent faults, and at the top of fold ridges. The fractures there are band-like around the Level 1 fracture development zone, with failure approach indices ranging from 1.456 to 1.568. Shear fractures are dominant, and they mainly strike northeast, northwest, and occasionally near-south–north.

(4) The Level III fracture development zone is mainly the structurally low parts in the northwest of the study area, except for the fracture zone and Level I and II fracture development zones. It covers an area larger than that of the Level II fracture development zone. The fractures in this zone are band-like in the northeastern and northwestern directions, with failure approach indices ranging from 0.816 to 1.037. Shear fractures are dominant, and they mainly strike northeast and northwest.

(5) The Level IV fracture-free zone has a limited fracture distribution, mainly in the northwest of the Level III fracture development zone in the Dingshan area. The rocks in this zone are rarely fractured, and the failure approach indices are <0.742. Fractures strike in a near-north–south direction.

The accuracy of the tectonic fracture predictions was verified by using the relative error (f). It is generally thought that if the relative error results do not exceed 25%, the prediction model is good and can be established, and the prediction results obtained for the fracture distribution are credible (Song et al., 2010; Wang et al., 2017).

The relative error formula is

$$f = \frac{|\text{Predicted - Measured}|}{\text{Predicted}} \times 100\% \quad . \tag{5}$$

Through analysis and comparison of the actual measured values of the fracture densities with the predicted densities of the Longmaxi Formation in the Dingshan area, the relative errors for all wells in the Dingshan area were found to be within 20% (Table 4). The actual measured values basically coincided with the observed values, and the overall conformity was very good. The fracture distribution prediction results were satisfactory and credible.

The paper insight from FEM numerical simulation method combined with rock strength failure criterion to predict the fracture distribution.The methodology described in this paper considers the spatial variations in mechanical parameters, the spatial changes in geological

Table 4 Analysis of the fracture predictive relative error of the Longmaxi Formation in the Dingshan area

Well number	DY4	DY3	DY2	DS1	DY1
Practical density (bar/m)	1.1	1.5	0.9	1.7	1.6
Predictive density (bar/m)	0.9	1.34	0.85	1.56	1.61
relative error (%)	18.2	10.6	5.6	14	0.63

structures. This method is suitable for not only shale reservoirs but also tight reservoirs and other low-permeability reservoirs. In these reservoirs, fracture zones are very important for the exploration and development of oil and gas fields.

6 Conclusions

The northeastern fault system is relatively developed in the Longmaxi Formation, Dingshan Area. Fractures primarily have either low angles or high angles, which can be attributed to the compression resulfted from the tectonic stress in the late Yanshanian to middle Himalayan tectonic movement. Fractures are generally 10–20 cm long and 0.1–1 mm wide and have high filling degree.

3-D finite element simulation technology was used to simulate the tectonic stress field in the study area, which involves rock mechanical experimental parameters and geostress data. Fault zones are weakened, whereas fold zones are strengthened, which enable the results of the simulation calculations and fracture predictions to be closer to the actual geological conditions. According to the obtained tectonic stress field distribution, the maximum principle stresses are evenly distributed within the range of −151.80 to −343.6 MPa, while the minimum principle stresses vary from −32.75 MPa to −181.3 MPa.

Based on the tectonic stress field analysis, rock fracture intensity was simulated, and the fracture development areas were predicted according to the rock failure criterion. It was found that the strongly fractured zones correspond to the Level I fracture development zone, which is the favorable zone for tectonic fracture formation and are mainly distributed in the vicinity of fault zones and the structurally high areas in the southeast. In addition, the moderately fractured zones correspond to the Level II fracture development zone and are mainly distributed in the periphery of the Level I fracture development zone. Both the Level I and Level II fracture development zones are regarded as favorable zones in the fracture predictions.

Acknowledgements

This research was supported by the Open Fund (PLN 201718) of State Key Laboratory of Oil and Gas Reservoir Geology and Exploitation, Southwest Petroleum University and the Open Fund (SEC-2018-04) of Collaborative Innovation Center of Shale Gas Resources and Environment, Southwest Petroleum University and the National Science and Technology Major Project of China (2017ZX05036003-003). The authors would like to thank the staff of all of the laboratories that cooperated in performing the tests and analyses.

Manuscript received May 24, 2018
accepted Dec 25, 2018
associate EIC HAO Ziguo
edited by Fei Hongcai

References

Cao, Z.L., Zheng, H.J., Gou, Y.C., Yuan, J.Y., Zhao, Y.C., and Shi, Y.M., 2009. Method of prediction and application on stochastical simulating 3D parameter field of rock mechanics. Geoscience, 6: 1126–1130.

Ding, W.L., Fan, T.L., Huang, X.B., and Li, C.Y., 2011. Upper Ordovician paleo tectonic stress field simulating and fracture distribution forecasting in Tazhong area of Tarim Basin, Xinjiang, China. Geological Bulletin of China, 30(4): 588–594.

Ding, W.L., Fan, T.L., Huang, X.B., and Liu, C., 2010. Paleo-structural stress field simulation for middle-lower Ordovician in Tazhong area and favorable area prediction of fractured reservoirs. Journal of China University of Petroleum (Edition of Natural Science), 34(5): 1–6.

Ding, W.L., Zeng, W.T., Wang, R.Y., Jiu, K., Wang, Z., Sun, Y.X., and Wang, X.H., 2016. Method and application of tectonic stress field simulation and fracture distribution prediction in shale reservoir. Earth Science Frontiers, 23(2): 63–74.

Dong, S.Q., Zeng, L.B., Cao, H., Xu, C.S., Wang, S.J., 2018. Principle and implementation of discrete fracture network modeling controlled by fracture density. Geological Review, 64(5): 1302–1314.

Fan, C.H., Qin, Q.R., Hu, D.F., Wang, X.L., and Zhu, M.Y., 2018. Fractal characteristics of reservoir structural fracture: a case study of Xujiahe Formation in central Yuanba area, Sichuan Basin. Earth Sciences Research Journal, 22(2): 113–118.

Fang, H.H., Sang, S.X., Wang, J.L., Liu, S.Q., and Ju, W., 2017. Simulation of paleotectonic stress fields and distribution prediction of tectonic fractures at the Hudi Coal Mine, Qinshui Basin. Acta Geologica Sinica (English Edition), 91 (6): 2007–2023.

Huang, R.C., Wei, X.F., and Wang, Q., 2017. Key factors of shale gas accumulation in Dingshan area of Southeastern Sichuan Basin. Marine Origin Petroleum Geology, 22(02): 25 –30.

Liu, C., Huang, X.B., Fan, T.L., Wang, Z.X., and Zeng, Q.B., 2008. The simulation of present tectonic stress field and the prediction of tectonic fractures of Ordovician in Tazhong area, Tarim Basin. Xinjiang Petroleum Geology, 2(4): 475–477.

Liu, C.R., 2002. Numerical simulation of Himalayan Epoch tectonic sress field in West Sichuan depression and its fracture prediction. Natural Gas Industry, (03): 10–13.

Lu, Y.X., Hu, W.S., Tang, J.G., Zhang, Q., Zhan, W., Xiong, P., and Lv, H.Y., 2016. Shale fracture development and distribution of Dingshan structural in Longmaxi formation of southeast Sichuan basin. Journal of Yangtze University (Natural Science Edition), 13(8): 6–10.

Lv, J., Zhou, W., Xie, R.C., Shan, Y.M., Zhang, C., and Xu, H., 2017. Three-dimensional in situ stress-field simulations of shale gas formations: A case study of the 5th Member of the Xujiahe Formation in the Xinchang gas field, West Sichuan Depression. Acta Geologica Sinica (English Edition), 91(2): 617–629.

Mei, L.F., Liu, Z.X., Tang, J.G. Shen, C.B., and Fan, Y.F., 2010. Mesozoic intra-continental progressive feformation in western Hunan-Hubei-eastern Sichuan Provinces of China: evidence from apatite fission track and balanced cross-section. Editorial Committee of Earth Science-Journal of China University of Geosciences, 35(2): 161–174.

Niu, W., Liang, J.P., Jiang, T., Sun, H., and Xie, X.Y., 2006. Fracture development characteristic and favorable zone prediction for Budatequn buried hill in Beier Depression. Petroleum Geology & Oilfield Development in Daqing, 25(4): 21–23.

Qin, Q.R., Zhang, L.H., Deng, H., Su, P.D., and Wang, Z.Y., 2004. Determination of magnitude of palaeo-tectonic stress and application to tectonic geological modeling. Chinese Journal of Rock Mechanics and Engineering, 23(23): 3979–3983.

Shen, G.H., 2008. Application of the finite element numerical simulation method in fracture prediction. Petroleum Geology and Recovery Efficiency, 15(4): 24–26.

Song, Y., Feng, J.W., Dai, J.S., Liu, X., Bian, B.L., and Li, M., 2010. Relationship between structural stress field and development of fractures foreland thrust belt. Journal of

Geomechanics,16(3): 310–324.
Tang, Y., Mei, L.F., Chen, Y.Z., Tang, W.J., Xiao, A.C., 2012. Controlling of structural stress field to the fractures in XuanHan-Daxian region,Northeastern Sichuan basin, China. Journal of Geomechanics, 18(2): 120–139.
Wang, B.F., Dai, J.S., Sheng, X.X., Qiao, C.L., and Li, J.P., 2009. Reservoir fracture forecast of mid-Shasan member in Niu 35 fault block. Journal of China University of Petroleum (Edition of Natural Science), 33(3): 18–26.
Wang, J.Y., Ju, W., Shen, J., Sun, W.F., 2016. Quantitative prediction of tectonic fracture distribution in the Chang 71 reservoirs of the Yanchang Formation in the Dingbian area, Ordos Basin. Geology and Exploration, 52(5): 966–973.
Wang, W.H., Li, K., Qin, Y.G., Yan, Z., and Tang, X., 2017. Method of prediction and application on stochastical simulating 3D parameter field of rock mechanics. Journal of Hefei University of Technology (Natural Science), 10: 1389–1393.
Wei, C.G., Lei, M.S., Wan, T.F., and Jie, W.Q., 2006. Numerical simulation of palaeotectonic stress field of Yingcheng Fm in Gulong- Xujiaweizi area: prediction and comparative study of tectoclase development area. Oil & Gas Geology, 27(1): 78–84.
Wei, J., and Sun, W.F., 2016. Tectonic fractures in the Lower Cretaceous Xiagou Formation of Qingxi Oilfield, Jiuxi Basin, NW China. Part two: Numerical simulation of tectonic stress field and prediction of tectonic fractures. Journal of Petroleum Science and Engineering,146: 626–636.
Wei, X.F., Zhao, Z.B., Wang, Q.B., Liu, Z.J., Zhou, M., and Zhang, H.,2017. Comprehensive evaluation on geological conditions of the shale gas in upper Ordovician Wufeng Formation-lower Silurian Longmaxi Formation in Dingshan Area, Qijiang, Southeastern Sichuan. Geological Review, 63 (1): 153–164.
Xie, R.C., Zhou, W., Tao, Y., Wang, S.Z., Yao, J., and Deng, H., 2008. Application of finite element analysis in the simulation of the in-situ stress field. Petroleum Drilling Techniques, 36 (2): 60–63.
Yin, S., Shan, Y.M., Ding, Z.W., Wang, W.L., Wang, J.Q., Li, R.B., and Liu, Y.F., 2014. Fracture criterion equation in the application of deep rock mechanics intensity response. Progress in Geophysics, (6): 2942–2949.
You, G.F., 2010. Reservoir fracture prediction of three-dimensional finite element numerical simulation. Chengdu University of Technology.
Yuan, H.F., 2008. The Mechanism of Hydrocarbon Accumulation, Sinian-Lower Palaeozoic, Sichuan Basin. Chengdu University of Technology.
Yuan, L.L., 2014. The Analysis of main controlling factors and development characteristics of Permian shale cracks in Chaobei District. China University of Mining and Technology.
Zeng, W.T., Ding, W.L., Zhang, J.C., Zhang, Y.Q., Guo, L., Jiu, K., and Li, Y.f., 2013. Fracture development in Paleozoic shale of Chongqing area (South China). Part two: Numerical simulation of tectonic stress field and prediction of fractures distribution. Journal of Asian Earth Sciences,75: 267–279.
Zhang, L.Y., Zhuo, X.Z., Ma, L.C., Chen, X.S., Song, L,C., and Zhou, X.G., 2015. Application of pore evolution and fracture development coupled models in the Prediction of reservoir “Sweet Spots” in tight sandstones. Acta Geologica Sinica (English Edition), 89(3): 1051–1052.
Zhang, S.J., 2014. Structural characteristics and its control of of the fracture of shales in the Longmaxi Formation, in southeastern Chongqing. China University of Mining and Technology.
Zhang, S.R., Wan, T.F., and Chen, J.P., 2004. Tectonic stress field modeling and fracture prediction in T3x2-4 strata in Xiaoquan-Xinchang area, western Sichuan depression. Oil & Gas Geology, 25(1): 70–74.
Zhou, Z.L., and You, G.F., 2009. Study on three-dimensional finite element numerical simulation. Journal of Harbin University of Commerce, 25(6): 737–740.
Zhou, X.G., Zhang, L.R., Zhang, M.L., Yuan, J.Y., Huang, F., and Liang, Y.P., 2003. Fractural distribution and reservoir-formed stress field in medium buried hill zone of Huanxiling Oilfield. Xinjiang Petroleum Geology, 24(1): 50–54.
Zhu, D.W., 2013. Developmental characteristics, major regulating factors and distribution prediction of fractures in shale of upper Triassic Yangchang Formation in Yangchang Oil-Gas Field. China University of Geosciences (Bejing).

About the first and corresponding author

XIE Jiatong Female; born in 1992 in Daqing City, Heilongjiang Province; Ph. D. candidate majoring in Geological Resources and Geological Engineering, Southwest University of Petroleum; She is mainly engaged in fracture development and reservoir formation work.E-mail: 963955769@qq.com; phone:13980941404.